J Fluoresc
DOI 10.1007/s10895-017-2155-6

ORIGINAL ARTICLE

Spectral, Electrochemical and Computational Investigations of Binding of n-(4-Hydroxyphenyl)-imidazole with p-Sulfonatocalix[4]arene

Marimuthu Senthilkumaran[1] · Kalimuthu Maruthanayagam[1] · Ganesan Vigneshkumar[1] · Ramesh Kumar Chitumalla[2] · Joonkyung Jang[2] · Paulpandian Muthu Mareeswaran[1]

Received: 30 May 2017 / Accepted: 31 July 2017

Abstract The interaction of n-(4-hydroxyphenyl)-imidazole with p-sulfonatocalix[4]arene is studied using fluorescence technique. The quenching of fluorescence intensity explains the efficiency of binding via binding constant and quenching constant. The excited state lifetime of n-(4-hydroxyphenyl)-imidazole is decreased upon interaction with p-sulfonatocalix[4]arene. The cyclic voltametric studies emphasized the interaction of n-(4-hydroxyphenyl)-imidazole with p-sulfonatocalix[4]arene. Quantum chemical calculations are carried out to study the interactions as well as charge transfer between the host and the guest upon complexation. The simulations revealed that the n-(4-hydroxyphenyl)-imidazole interacts with p-sulfonatocalix[4]arene with horizontal orientation with in the p-sulfonatocalix[4]arene cavity.

Keywords p-Sulfonatocalix[4]arene · Imidazole · Fluorescence · Excite state lifetime · Cyclic voltammetry · Computational calculations

Marimuthu Senthilkumaran and Kalimuthu Maruthanayagam contributed equally to this manuscript.

Electronic supplementary material The online version of this article (doi:10.1007/s10895-017-2155-6) contains supplementary material, which is available to authorized users.

✉ Joonkyung Jang
jkjang@pusan.ac.kr

✉ Paulpandian Muthu Mareeswaran
mareeswaran@alagappauniversity.ac.in;
muthumareeswaran@gmail.com

[1] Department of Industrial Chemistry, Alagappa University, Karaikudi 630 003, India

[2] Department of Nanoenergy Engineering, Pusan National University, Busan 609-735, South Korea

Introduction

Water soluble macrocyclic molecules are most attractive molecules to study host–guest interactions both in solution and solid state [1, 2]. Water soluble calixarenes have extensive applications like drug delivery, molecular recognition, and crystal engineering [3–9]. The sulfonation of *tert*-butylcalix[4]arene on para position renders highly water-soluble p-sulfonatocalix[4]arene (p-SC4) [10]. The cone shaped structure of p-SC4 is stabilized by intramolecular hydrogen bonding at the lower rim [11]. The p-SC4 have hydrophobic (aromatic rings) cavity and hydrophilic (sulphonato and hydroxyl groups) rims [12]. The uniqueness of p-SC4 is the flexible cavity structure due to the phenolic rings interconnected by means of methylene bridge, compared to other water soluble host molecules like cyclodextrins and cucurbiturils [13]. This uniqueness makes p-SC4 efficient to encapsulate simple organic molecules [14–16], ionic compounds [17], biologically important macromolecules, peptides and proteins [18]. There are numerous reports on the host–guest chemistry of p-SC4 with drug molecules [19, 20] like lomefloxacin [21], 9-amino-acridine [22], vitamin K3 [23], Norfloxacin [24]. Kahwajy et al. studied binding of the anticancer drug (phenanthriplatin) with cucurbit[n]urils, β-cyclodextrin and p-SC4. They reported that the p-SC4 was the efficient drug delivery vehicle among the other macrocycle molecules [12].

The n-(4-hydroxylphenyl) imidazole (NHIP) contains two functional aromatic moieties (phenolic and imidazole group) (Fig. 1). The encapsulation of one particular functional group is one of the strategy to explore the functionalities of the other group while both groups are present in the same molecule [25]. The imidazole group is having very important role in biology [26, 27]. Imidazole is one of the active centers of proteins, it can cleave DNA efficiently in the

Published online: 08 September 2017

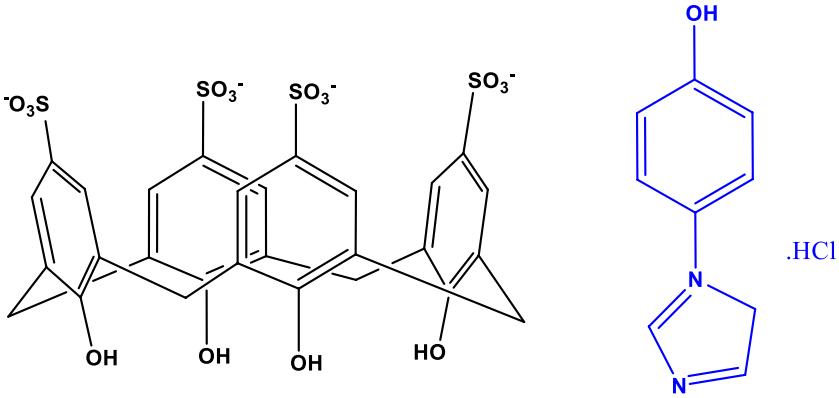

Fig. 1 Structure of p-Sulfonatocalix[4]arene (p-SC4) and N-(4-hydroxylphenyl) imidazole (NHIP)

physiological environment [28, 29]. Feng et al. studied the interaction between cucurbit[n]urils ($n = 6,7,8$) with some imidazole derivatives and reported in presence of cucurbit[n] urils the phenyl group of NHIP inside the cavity of and imidazole group outside of the cavity [26]. Huo et al. reported the NHIP containing complex with cucurbit [6]uril and studied DNA cleavage in physiological environment [30]. In this present work, the host–guest interaction between NHIP with p-SC4 in an aqueous medium, using emission, excited lifetime, electrochemical methods are studied. Density functional theory (DFT) based theoretical simulations employed to investigate the interaction energies and orientations of NHIP with p-SC4. The DFT simulations revealed the charge transfer phenomenon upon complexation.

Experimental Section

Materials

N-(4-hydroxylphenyl) imidazole and t-butylcalix[4]arene are procured from Sigma–Aldrich. Hydrochloric acid is purchased from Fisher Scientific. Ultra-pure water (Millipore) and ethanol are used as solvent throughout the study. p-SC4 is synthesized according to the reported procedure [31]. The NHIP, as such, is not soluble in water, therefore, NHIP is converted to hydrochloride salt using literature procedure [26].

Instruments

The emission measurements are performed by using JASCO FP-8200 Spectrofluorometer at room temperature. The excited state fluorescence lifetime is measured using time correlated single photon counting method (TCSPC) in HORIBA JOBIN-VYON data station. The electrochemical studies are carried out using Auto lab electrochemical analyzer (GPES software). A classical three electrode cell assembly is used for the electrochemical measurements. Cyclic Voltammetry measurements are carried out using glassy carbon electrode with diameter 3 mm as working electrode at applied potential from − 1.3 to 1.2 V for each sample with single cycle. The reference electrode is saturated calomel electrode (SCE) and the platinum electrode is the counter electrode. All experiments are carried out at 30 ± 1 °C. The working electrode is polished well to a mirror with 0.05 µm alumina aqueous slurry, and washed with double distilled water before performing each experiment. The FT-IR spectra are recorded on Jasco FTIR 4600 spectrometer using KBr pallets in the range of $4000 - 400\ cm^{-1}$.

Fluorescence Spectral Titration

The stock solution of 1.03×10^{-3} M is prepared in 25 ml SMF. The concentration of NHIP is fixed at 1×10^{-5} M, and the concentration of p-SC4s, is varied from 1×10^{-5} M to 5×10^{-5} M and the fluorescence spectra are recorded. The measurement of the binding constant is based on the changes in the fluorescence intensity with increasing concentration of p-SC4 [11]. The binding constant is calculated using Eq. (1).

$$\log\left[\left(F_0 - F\right)/F\right] = n \log [H] + \log K_a \quad (1)$$

Where F_0 is the fluorescence intensity of NHIP in the absence of p-SC4, F is the fluorescence intensity in the presence of various concentrations of p-SC4, [H] is the concentration of p-SC4, K_a is the binding constant, n is the stoichiometric ratio.

The quenching constant, k_q is calculated by using the Stern–Volmer equation [30], Eq. (2).

$$F_0/F = 1 + k_q \tau [p - SC4] \quad (2)$$

The determination of thermodynamic parameters in the host–guest complex is the free energy change of a reaction. It can be calculated from the binding constant value using the following Eq. (3)

$$\Delta G = -RT \ln K_a \quad (3)$$

where, ΔG is the free energy change of the reaction, R is gas constant, T is temperature and 'K_a' is binding constant.

Fluorescence Lifetime

The excited state fluorescence lifetime is measured using time correlated single photon counting method (TCSPC). The pulsed-diode LED at 280 nm is used as light source to excite the molecule. The pulse-width is about 1.4 ns with an upper repetition rate of 1 MHz [32]. The concentration of NHIP is fixed (1×10^{-4} M), the concentration of p-SC4 is varied ($0.5\times10^{-4}-2\times10^{-4}$ M) and the excited state lifetime is recorded for these samples. The data generated is used to plot decay versus time. From the plot, the lifetime is calculated.

Cyclic Voltammetry (CV) Studies

The aqueous solution of 1×10^{-3} M of NHIP and p-SC4 are prepared seperately. The 10 ml of p-SC4 is taken in three electrode cell setup and CV is performed. Then increamental additions of 2 ml of NHIP is added and CV is recoreded. This procedure is continued up to 10 ml of NHIP so that the concentration will reach to 1:1 ratio. The above procedure is repeated by fixing 10 ml of NIPH with 2 ml of increamental additions of p-SC4 up to 10 ml.The recorded CVs are used to calculate binding constant [33, 34]. The binding constant is calculated using Eq. (4).

$$1/\left(I_{HG}-I_G\right)=1/\Delta I+1/K_a[NHIP]_0\Delta I\left[p-SC4\right]_0 \quad (4)$$

Where I_G is the oxidation peak current of guest molecule of NHIP, and I_{HG} is the oxidation peak current of inclusion complex of NHIP with p-SC4. $I_{HG}-I_G$ means the peak current difference between inclusion complex and guest molecule. ΔI is the difference between the molar peak current coefficient of the inclusion complex and NHIP; $[NHIP]_0$ and $[p\text{-}SC4]_0$ are the initial concentration of NHIP and p-SC4, respectively.

Sample Preparation for FT-IR Spectroscopy

The solid state inclusion complex is prepared using co-evaporation method. The p-SC4 (0.1 g) and NHIP (0.0193 g) having 1:1 ratio is taken in 5 ml of water in a 50 ml beaker and sonicated for 1 h. After getting a clear solution the mixture is evaporated to dryness. The sample is further dried under vacuum to remove traces of water. The dried solid is used in the FT-IR spectral study.

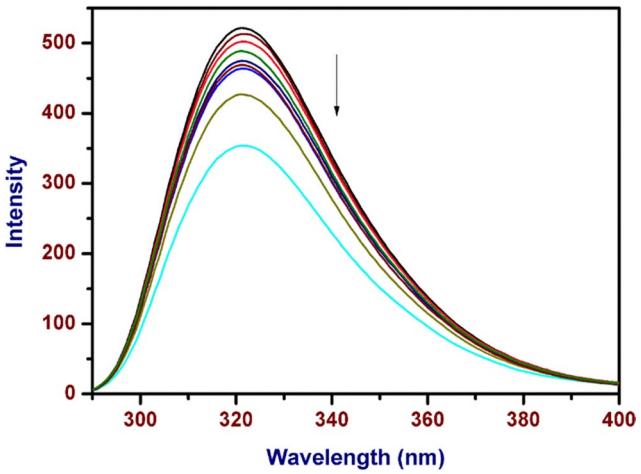

Fig. 2 Emission spectrum of NHIP (1×10^{-5} M) in absence and presence of varies concentration (1×10^{-5} M to 5×10^{-5} M) of p-SC4

Computational Details

All the calculations reported in this paper are performed with Gaussian 09 quantum chemical software package [35]. No symmetry constraints are imposed during the optimization of either individual fragments of complexes. The simulations are carried out in the gas phase. We used a hybrid meta-GGA based Minnesota functional (M06-2X) [36] along with the 6-31g(d) basis set. The chosen functional is ideal for studying the non-covalent interactions. The vibrational frequency analysis is performed upon optimized geometries. The absence of imaginary frequencies confirms the local minima of each structure on their respective potential energy surfaces. The interaction

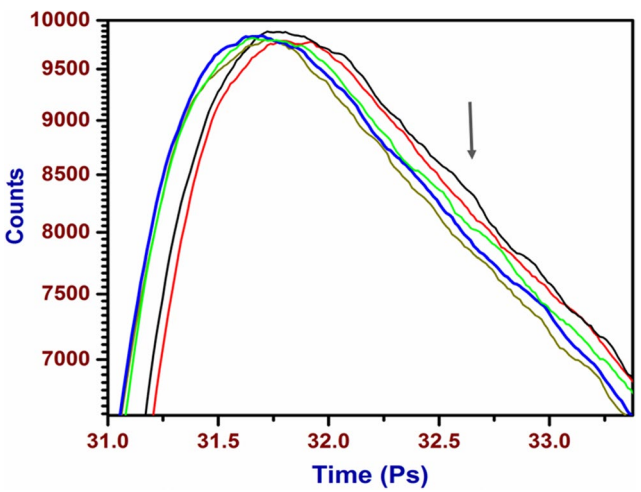

Fig. 3 Excited state lifetime spectrum of NHIP (1×10^{-4} M) (Block) with increasing addition of p-SC4 (0.5×10^{-4} M to 2×10^{-4} M)

Table 1 Excited state lifetime of NHIP with various concentration p-SC4

S. no	Concentration of p-SC4	Lifetime (τ) Ps
1	0	770.474
2	0.5×10^{-4} M	770.195
3	1×10^{-4} M	769.455
4	1.5×10^{-4} M	767.182
5	2×10^{-4} M	763.611

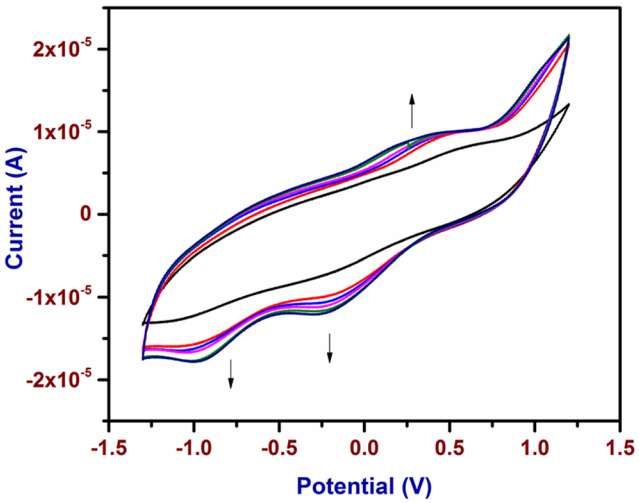

Fig. 4 CV of p-SC4 (10 ml of 10^{-3} M) with addition of increasing volume of NHIP

energies reported in this paper are corrected for basis set superposition error (BSSE) [37].

Results and Discussion

Fluorescence Titration Study

The fluorescence spectra of NHIP is shown in Figure S1. The emission maxima of NHIP is 321 nm with excitation at 280 nm. The p-SC4 is not having fluorescent property. Therefore, the fluorescence is a suitable method to study

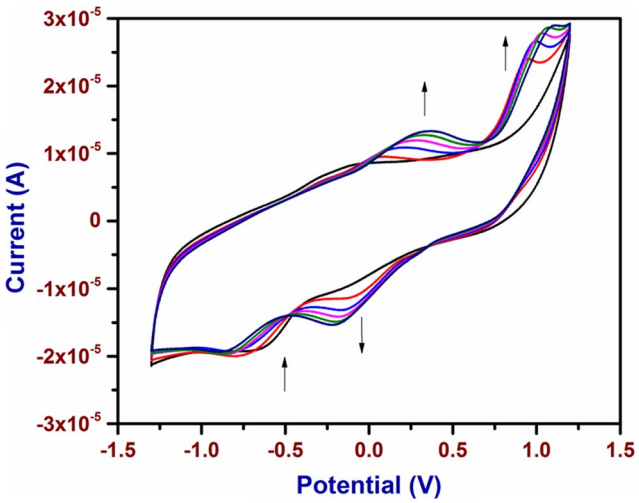

Fig. 5 CV of NHIP (10 ml of 10^{-3} M) with addition of increasing volume of p-SC4

the interaction between NHIP and p-SC4. The concentration of NHIP is fixed, the concentration of p-SC4 is varied as given in the Experimental section and the emission spectra is recorded. The emission spectrum of NHIP with various concentrations of p-SC4 is shown in Fig. 2. The emission intensity of NHIP is quenched in the presence of increasing concentration of p-SC4. The quenching is due to the binding of NHIP with p-SC4. The binding constant is calculated using the modified Stern–Volmer plot (Figure S2). The binding constant value calculated from Eq. 1 is 2.2×10^{4} M^{-1}. The binding constant value exhibits strong binding between NHIP and p-SC4. The quenching constant is also calculated using Stern–Volmer equation (Eq. 2). The Stern Volmer plot is given in Figure S3 and the quenching constant calculated is 3.3×10^{12} M^{-1} S^{-1}. This quenching constant value confirms the static quenching due to the ground state complex formation.

The binding ratio of NHIP-p-SC4 host–guest complex is studied using Job's method. The concentration of NHIP is varied from 1×10^{-5} M to 9×10^{-5} M and the p-SC4 concentration is in the reverse order from 9×10^{-5} M to 1×10^{-5} M. The mole fraction is plotted with the emission intensity change (Figure S4). The Job's plot confirms

Table 2 Oxidation and reduction peak of p-SC4 changes with addition of NHIP

S. no	Concentration of p-SC4 (ml, 10^{-3} M)	E_{pa} (V)	I_{pa} (A)	$E_{pc}{}^{1}$ (V)	$I_{pc}{}^{1}$ (A)	$E_{pc}{}^{2}$ (V)	$I_{pc}{}^{2}$ (A)
1	0	0.594	8.135×10^{-6}	–	–	–	
2	2	0.429	9.048×10^{-6}	−0.203	-9.917×10^{-6}	−0.986	-15.619×10^{-6}
3	4	0.409	9.371×10^{6}	−0.203	10.469×10^{-6}	−0.982	-15.982×10^{-6}
4	6	0.389	9.431×10^{-6}	−0.206	-11.021×10^{-6}	−0.968	-16.539×10^{-6}
5	8	0.376	9.482×10^{-6}	−0.221	-11.573×10^{-6}	−0.968	-17.642×10^{-6}
6	10	0.372	9.607×10^{-6}	−0.248	11.941×10^{-6}	−0.968	-17.642×10^{-6}

Table 3 Reduction peak of NHIP changes with addition of p-SC4

S. no	Concentration of NHIP (ml, 10^{-3} M)	E_{pc}^{1} (V)	I_{pc}^{1} (A)	E_{pc}^{2} (V)	I_{pc}^{2} (A)
1	0	−0.168	-9.966×10^{-6}	−0.613	-18.573×10^{-6}
2	2	−0.124	-11.291×10^{-6}	−0.783	-19.677×10^{-6}
3	4	−0.151	-13.056×10^{-6}	−0.811	-19.531×10^{-6}
4	6	−0.168	-14.159×10^{-6}	−0.821	-19.361×10^{-6}
5	8	−0.101	-15.042×10^{-6}	−0.842	-19.124×10^{-6}
6	10	−0.213	-15.488×10^{-6}	−0.841	-19.124×10^{-6}

the 1:1 binding of NHIP with p-SC4. The free energy change (ΔG) of host–guest complex calculated using Eq. 3 is −25.2 KJ mol^{-1}. The negative ΔG value indicates that the host–guest complexation process is spontaneous.

Excited State Lifetime Using TCSPC

The excited state lifetime of NHIP is 770.474 Ps. The concentration NHIP is fixed at 1×10^{-4} M, the p-SC4 concentration is varied from 0.5×10^{-4} M to 2×10^{-4} M and the excited state lifetime is recorded. The decrease in the lifetime is observed by increasing concentration of p-SC4. The changes in the fluorescence decay are shown in Fig. 3 and the lifetime data is collected in Table 1. The decrease of fluorescence lifetime is due the binding of NHIP with p-SC4.

Electrochemical Properties

The cyclic voltammogram of p-SC4 is shown in Figure S4. The shoulder peak around 0.8 V, is the oxidation of phenolic moiety present in the p-SC4 [38]. The 1×10^{-3} M of 10 ml of p-SC4 is taken in the cell setup. The 2 ml of incremental additions of NHIP is added to the p-SC4 and CV is recorded for each addition. The oxidation peaks current (around 0.8 V) is increased and shifted to zero potential and the reduction peak at −0.215 and 0.955 V appeared (Fig. 4), these changes are due to the formation of the inclusion complex between NHIP and p-SC4. The peak potential and peak current values of each addition is collected Table 2. The binding constant is calculated using Benesi–Hildebrand method (Eq. 4). The binding constant is calculated using Benesi–Hildebrand plot (Figure S6) and the binding constant value is 2.6×10^{2} M^{-1}.

The CV of NHIP is shown Figure S7. This figure shows one oxidation peak (−0.145 V) and two reduction peaks (−0.168 and −0.613 V). The peak −0.613 V is due to the presence of imidazole group present in NHIP [39]. The 1×10^{-3} M of 10 ml NHIP is fixed and the 2 ml incremental addition of p-SC4 are added and CV is recorded (Fig. 5). A

Table 4 Oxidation peak of NHIP changes with addition of p-SC4

S. no	Concentration of NHIP (ml, 10^{-3} M)	E_{pa}^{1} (V)	I_{pa}^{1} (A)	E_{pa}^{2} (V)	I_{pa}^{2} (A)
1	0	−0.145	8.081×10^{-6}	–	–
2	2	0.075	9.371×10^{-6}	0.956	23.831×10^{-6}
3	4	0.155	10.913×10^{-6}	0.982	26.553×10^{-6}
4	6	0.199	11.572×10^{-6}	1.012	27.281×10^{-6}
5	8	0.261	12.686×10^{-6}	1.047	28.281×10^{-6}
6	10	0.297	$13.12\,4\times10^{-6}$	1.074	28.692×10^{-6}

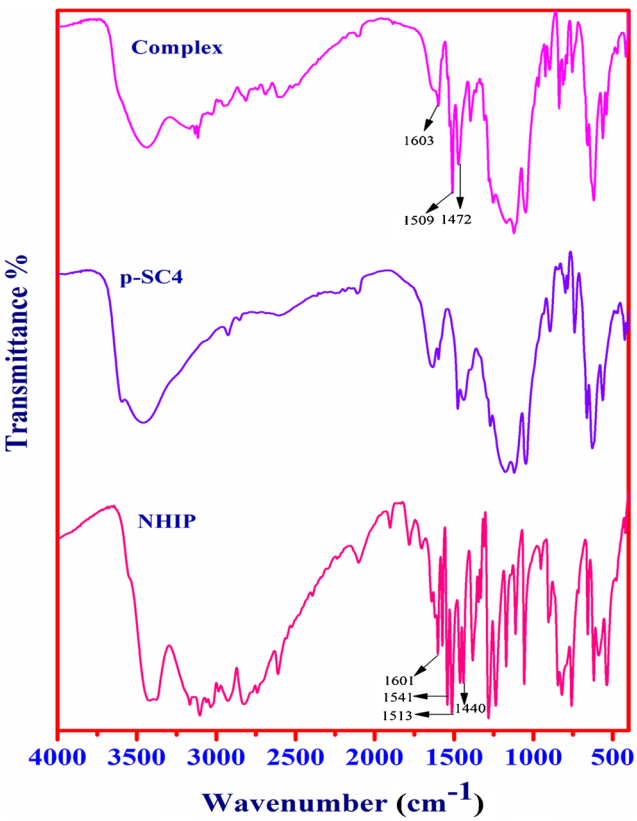

Fig. 6 FT-IR spectra of p-SC4, NHIP and p-SC4-NHIP complex

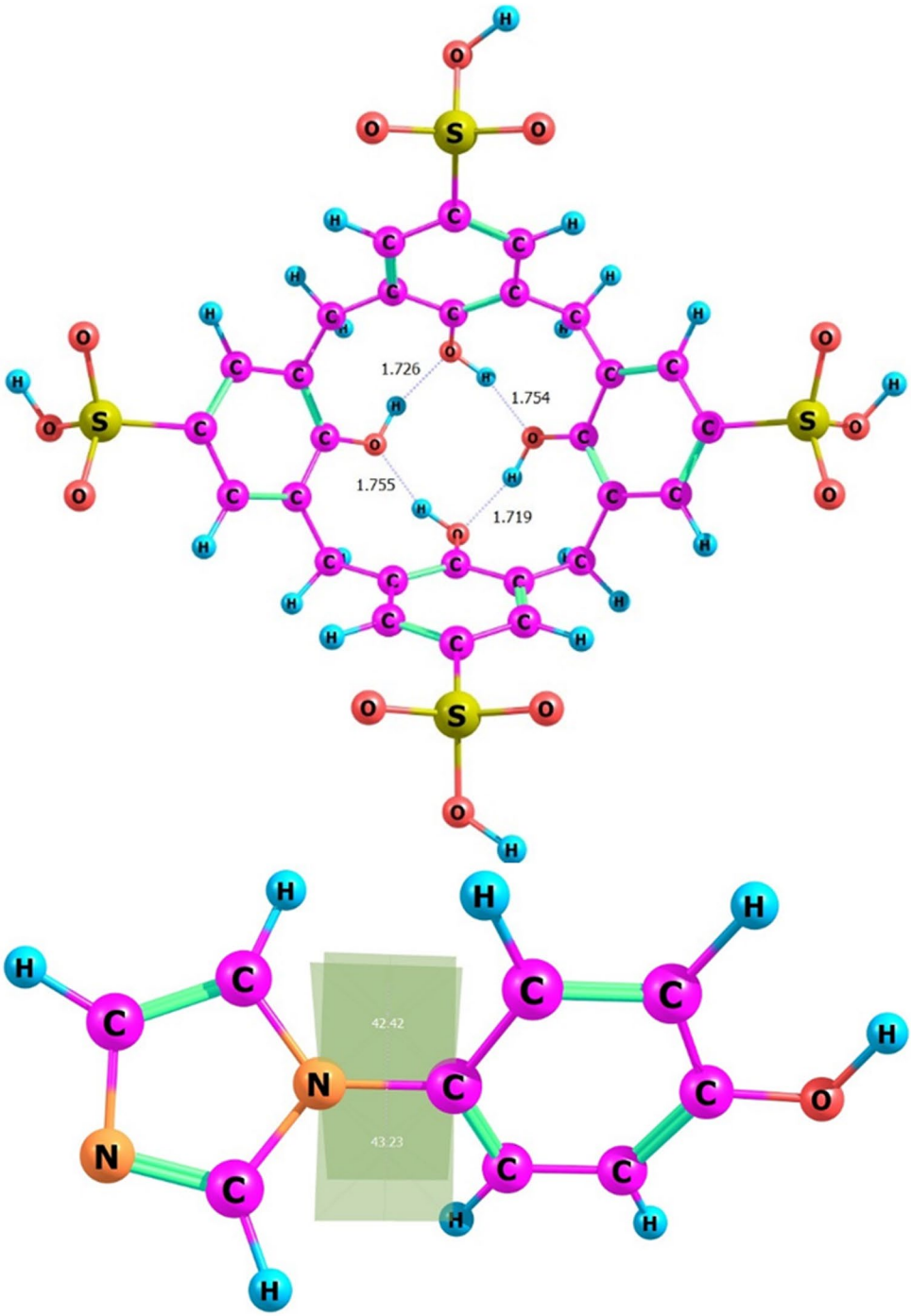

Fig. 7 The optimized geometries of p-SC4 (top) and NHIP (bottom) obtained at M06-2X/6-31G(d) level of the theory

new oxidation peak at 0.95 V is observed and the reduction peak at − 0.613 V is decreased. The oxidation peak is due to the –OH group present in the p-SC4. The reduction peak at − 0.613 V is decreased further and moved to more negative side by addition of p-SC4. The electron density decreases due to the –OH of NHIP interact p-SC4 to form complex (Tables 3 and 4). The binding constant is calculated using Benesi–Hildebrand method (Eq. 4). The Benesi–Hildebrand plot is shown in Figure S8 and the binding constant value calculated is 7.6×10^2 M^{-1}.

FT-IR Spectral Studies

The FT-IR spectra of p-SC4, NHIP and p-SC4- NHIP inclusion complex are shown in Fig. 6. The peak at 1601 cm^{-1} is due to the –C–C– of imidazole ring and the peaks at 1541 cm^{-1}, 1513 cm^{-1}, 1440 cm^{-1} are due to the C–N. The peaks at 1541 cm^{-1}, 1440 cm^{-1} are disappeared and 1513 cm^{-1} is shifted to 1509 cm^{-1}. These changes are attributed to the interaction imidazole group of NHIP to the p-SC4 cavity. These results resembles our previous reports

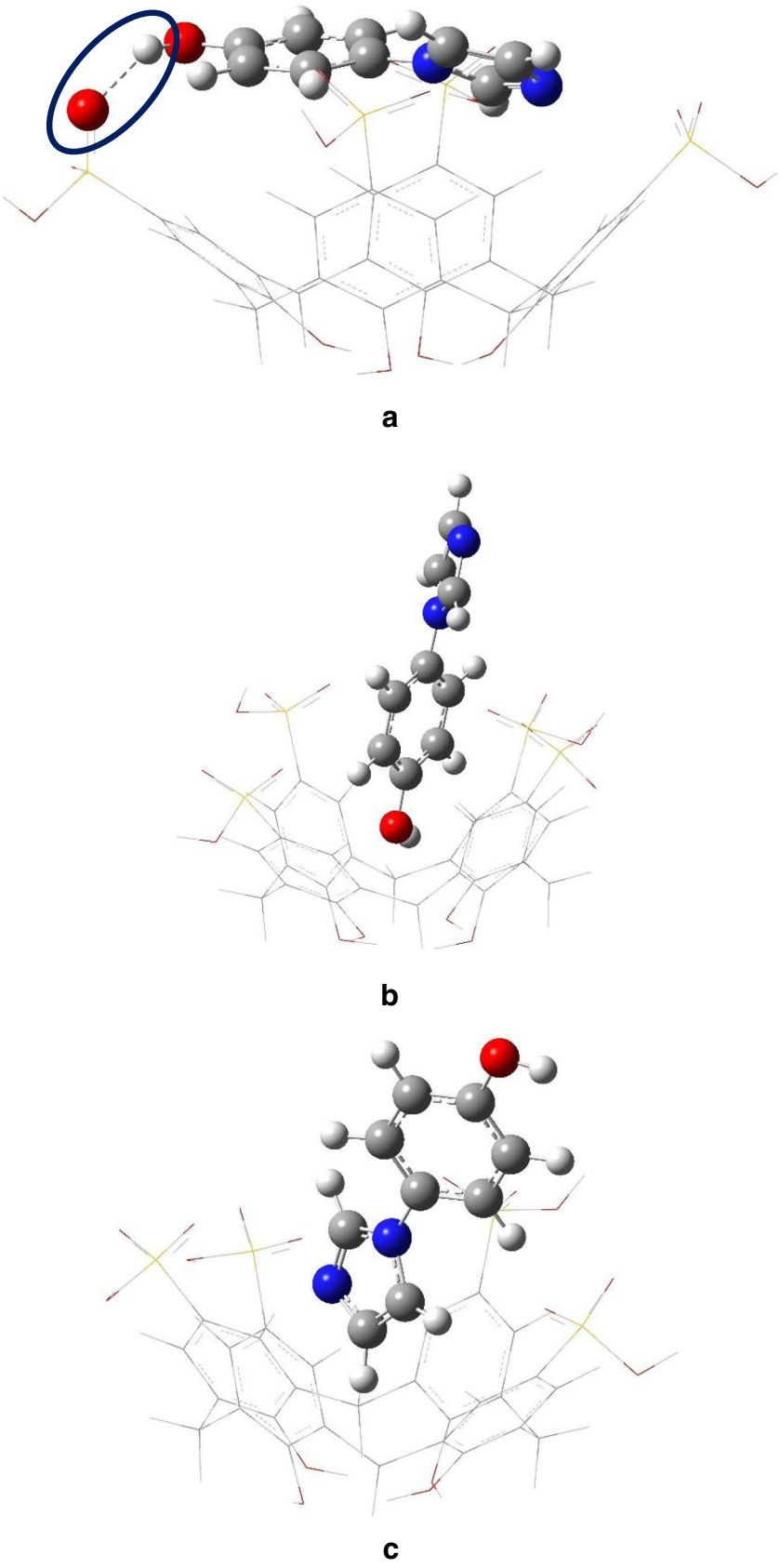

Fig. 8 The optimized geometries of the complexes p-SC4-NHIP. The NHIP is oriented in **a** Horizontal, **b** Vertical-1 and **c** Vertical-2. The hydrogen bond is shown in the circle

Table 5 Simulated complexation energies and dipole moments of horizontally and vertically oriented NHIP with p-SC4 obtained at M06-2X/6-31G(d) level of the theory

p-SC4-NHIP	BSSE uncorrected (kcal/mol)	BSSE corrected (kcal/mol)	BSSE energy kcal/mol	Dipole moment (D)
Horizontal	− 28.53	− 18.99	9.54	13.44
Vertical-1	− 22.45	− 13.89	8.56	17.03
Vertical-2	− 25.78	− 16.93	8.85	12.52

of cavity binding of p-SC4 with respective guest molecules [40, 41]. The cavity binding of NHIP with p-SC4 is confirmed using FT-IR spectral studies.

Computational Studies

To further explore the interactions between NHIP and p-SC4, we make use of quantum chemical simulations. The calculations assisted in elucidating the most stable orientation of NHIP in the cavity of p-SC4 and to determine the interaction energy. In order to find the most stable orientation, we modeled three host–guest complexes. In the first model, the NHIP was oriented horizontally in the cavity of p-SC4. In the second model (Vertical-1), the NHIP is oriented vertically and the hydroxyphenyl ring placed inside the cavity of p-SC4. In the third model (Vertical-2) also the NHIP is oriented vertically but the imidazole ring is placed inside the cavity of p-SC4. The optimized structures of p-SC4 and NHIP are shown in Fig. 7 and the complexes are shown in Fig. 8. The simulated interaction energies of three modeled systems are compiled in Table 5. The interaction energy of NHIP with p-SC4 is more (− 18.99 kcal/mol) when it is oriented horizontally and this high interaction energy can be attributed to the H-bonding formed between the hydroxyl hydrogen of NHIP and one of the sulfonyl oxygen of p-SC4. The interaction energies are found to be − 13.89 and − 16.93 kcal/mol for vertical-1 and vertical-2 models, respectively. The negative sign of the interaction energy indicates the stabilization upon complexation. The BSSE uncorrected interaction energies and the dipole moments of the complexes were also given in the same table. For the most stable complex (model-1), we have carried out the population analysis to study the charge transfer phenomenon. In the HOMO of the complex, the electron density is fully localized over NHIP whereas in the LUMO the electron density is completely shifted to the p-SC4. The electron density distribution plots of the frontier molecular orbitals are given in Fig. 9. From the electron density distribution plots, it is clear that the charge transfer takes place from the NHIP to p-SC4 upon complexation.

Conclusion

The binding constant value of NHIP with p-SC4 using fluorescence technique is around $10^4\ M^{-1}$, confirms the efficient binding of NHIP with p-SC4. The quenching constant is also around $3.3 \times 10^{12}\ M^{-1}\ S^{-1}$ emphasized the presence of static quenching due to the ground state complex formation. The CV studies shows the changes in the redox behavior of NHIP in the presence of p-SC4. The binding constant value calculated using CV technique is around $10^2\ M^{-1}$. Since the fluorescence technique is more sensitive technique than electrochemical techniques the binding constant value from fluorescence technique is higher than the value from CV technique. The FT-IR spectral study confirms the cavity binding of NHIP with p-SC4. The DFT studies revealed that the NHIP binds strongly with p-SC4 in its horizontal orientation. The calculated electron density distribution plots confirm the charge transfer from NHIC to p-SC4 upon complexation.

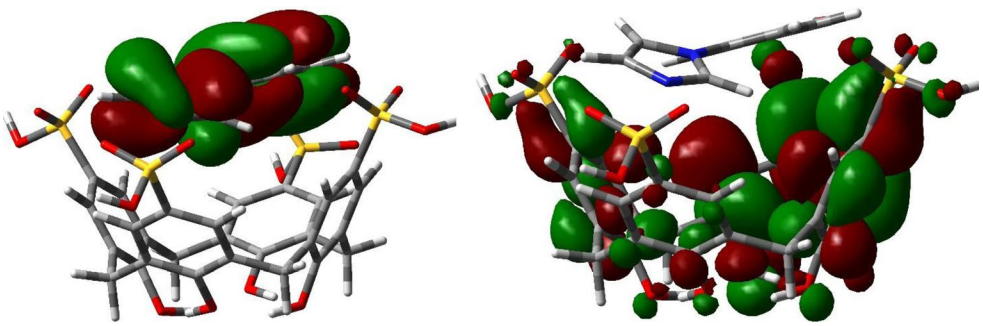

Fig. 9 The calculated charge transfer in frontier molecular orbitals of the complex p-SC4-NHIP

Acknowledgements Authors gratefully thank Department of science and Technology (DST INSPIRE) [Project number - IFA14/CH-147], India for financial support. This research was supported by Korea Research Fellowship program funded by the Ministry of Science, ICT and Future Planning through the National Research Foundation of Korea (2016H1D3A1936765).

References

1. Murray J, Kim K, Ogoshi T, Yao W, Gibb BC (2017) The aqueous supramolecular chemistry of cucurbit[n]urils, pillar[n]arenes and deep-cavity cavitands. Chem Soc Rev 46:2479–2496
2. Ma X, Zhao Y (2015) Biomedical applications of supramolecular systems based on host–guest interactions. Chem Rev 115:7794–7839
3. Rodik RV, Boyko VI, Kalchenko VI (2009) Calixarenes in biomedical researches. Curr Med Chem 16:1630–1655
4. Bombicz P, Gruber T, Fischer C, Weber E, Kálmán A (2014) Fine tuning of crystal architecture by intermolecular interactions: synthon engineering. CrystEngComm 16:3646–3654
5. Zhang F, Sun Y, Tian D, Shin WS, Kim JS, Li H (2016) Selective molecular recognition on calixarene-functionalized 3D surfaces. Chem Commun 52:12685–12693
6. Gutsche CD, Alam I (1988) Calixarenes. 23. The complexation and catalytic properties of water soluble calixarenes. Tetrahedron 44:4689–4694
7. Gutsche CD, Pagoria PF (1985) Calixarenes. 16. Functionalized calixarenes: the direct substitution route. J Org Chem 50:5795–5802
8. Madasamy K, Gopi S, Senthilkumaran S, Radhakrishnan S, Velayutham D, Muthu Mareeswaran P, Kathiresan M (2017) A supramolecular investigation on the interactions between ethyl terminated bis–viologen derivatives with sulfonato calix[4]arenes. Chem Select 2:1175–1182
9. Muthu Mareeswaran P, Ethiraj B, Veerasamy S, Kim B, Woo SI, Seenivasan R (2014) p-Sulfonatocalix[4]arene as carrier for curcumin. New J Chem 38:1336–1345
10. Shinkai S, Mori S, Tsubaki T, Sone T, Manabe O (1984) New water-soluble host molecules derived from calix [6] arene. Tetrahedron lett 25:5315–5318
11. Muthu Mareeswaran P, Prakash M, Subramanian V, Rajagopal S (2012) Recognition of aromatic amino acids and proteins with p-sulfonatocalix[4]arene—a luminescence and theoretical approach. J Phys Org Chem 25:1217–1227
12. Kahwajy N, Nematollahi A, Kim RR, Church WB, Wheate NJ (2017) Comparative macrocycle binding of the anticancer drug phenanthriplatin by cucurbit[n]urils, β-cyclodextrin and para-sulfonatocalix[4]arene: a 1 H NMR and molecular modelling study. J. Incl Phenom Macrocycl Chem 87:251–258
13. Guo D-S, Uzunova VD, Assaf KI, Lazar AI, Liu Y, Nau WM (2016) Inclusion of neutral guests by water-soluble macrocyclic hosts—a comparative thermodynamic investigation with cyclodextrins, calixarenes and cucurbiturils. Supramol Chem 28:384–395
14. Danylyuk O, Leśniewska B, Suwinska K, Matoussi N, Coleman AW (2010) Structural diversity in the crystalline complexes of para-sulfonato-calix[4]arene with bipyridinium derivatives. Cryst Growth Des 10:4542–4549
15. Wang K, Guo D-S, Zhang H-Q, Li D, Zheng X-L, Liu Y (2009) Highly effective binding of viologens by p-sulfonatocalixarenes for the treatment of viologen poisoning. J Med Chem 52:6402–6412
16. Chao J, Wang H, Song K, Wang Y, Zuo Y, Zhang L, Zhang B (2017) Host–guest inclusion system of ferulic acid with p-sulfonatocalix[n]arenes: preparation, characterization and antioxidant activity. J Mol Struct 1130:579–584
17. Miller-Shakesby DM, Burke BP, Nigam S, Stasiuk GJ, Prior TJ, Archibald SJ, Redshaw C (2016) Synthesis, structures and cytotoxicity studies of p-sulfonatocalix[4]arene lanthanide complexes. CrystEngComm 18:4977–4987
18. Coleman AW, Jebors S, Cecillon S, Perret P, Garin D, Marti-Battle D, Moulin M (2008) Toxicity and biodistribution of para-sulfonato-calix[4]arene in mice. New J Chem 32:780–782
19. Perret F, Lazar AN, Coleman AW (2006) Biochemistry of the para-sulfonato-calix[n]arenes. Chem Comm 0:2425–2438
20. Guo D-S, Liu Y (2014) Supramolecular chemistry of p-sulfonatocalix[n]arenes and its biological applications. Acc Chem Res 47:1925–1934
21. Zhou Y, Lu Q, Liu C, She S, Wang L (2005) A novel spectrofluorimetric method for determination of lomefloxacin based on supramolecular inclusion complex between it and p-sulfonated calyx[4]arene. Anal Chim Acta 552:152–159
22. Zhou Y, Lu Q, Liu C, She S, Wang L (2006) Study on the inclusion behavior of p-sulphonatocalix[4]arene with 9-amino-acridine by spectrofluorometric titrations. Spectrochim Acta A 63:423–426
23. Lu Q, Gu J, Yu H, Liu C, Wang L, Zhou Y (2007) Study on the inclusion interaction of p-sulfonated calix[n]arenes with Vitamin K3 using methylene blue as a spectral probe. Spectrochim Acta A 68:15–20
24. Lu Q, Zhou Y, Sun J, Wu L, Yu H, Xu H, Wang L (2007) Preparation and property screening of the solid inclusion complex of norfloxacin with p-sulfonated calix [4] arene. Comb Chem High Throughput Screen 10:480–485
25. Daze K, Hof F (2016) Molecular interaction and recognition. In: Encyclopedia of physical organic chemistry. Wiley. doi:10.1002/9781118468586.epoc3001
26. Feng Y, Xue S-F, Fan Z-F, Zhang Y-Q, Zhu Q-J, Tao Z (2009) Host–guest complexes of some cucurbit[n]urils with the hydrochloride salts of some imidazole derivatives. J Incl Phenom Macrocycl Chem 64:121
27. Yang X, Chen L, Liu Y, Yang Y, Chen T, Zheng W, Liu J, He QY (2012) Ruthenium methylimidazole complexes induced apoptosis in lung cancer A549 cells through intrinsic mitochondrial pathway. Biochimie 94:345–353
28. Myers RS, Amaro RE, Luthey-Schulten ZA, Davisson VJ (2005) Reaction coupling through interdomain contacts in imidazole glycerol phosphate synthase. BioChemistry 44:11974–11985
29. Torok I, Gajda T, Gyurcsik B, Toth GK, Peter A (1998) Metal complexes of imidazole ligands containing histamine-like donor sets: equilibrium, solution structure and hydrolytic activity. J Chem Soc Dalton Trans 0:1205–1212
30. Huo F-J, Yin C-X, Yang P (2007) The crystal structure, self-assembly, DNA-binding and cleavage studies of the [2]pseudorotaxane composed of cucurbit[6]uril. Bioorg Med Chem Lett 17:932–936
31. Shinkai S, Araki K, Matsuda T, Nishiyama N, Ikeda H, Takasu I, Iwamoto M (1990) NMR and crystallographic studies of a p-sulfonatocalix (4) arene-guest complex. J Am Chem Soc 112:9053
32. Lakowicz JR (2007) Principles of fluorescence spectroscopy. Springer, New York
33. Srinivasan K, Stalin T, Sivakumar K (2012) Spectral and electrochemical study of host–guest inclusion complex between 2,4-dinitrophenol and β-cyclodextrin. Spectrochim Acta A 94:89–100
34. Saravanan C, Senthilkumaran M, Ashwin BM, Suresh P, Muthu Mareeswaran P (2017) Spectral and electrochemical investigation of 1,8-diaminonaphthalene upon encapsulation of p-sulfonatocalix[4]arene. J Incl Phenom Macrocycl Chem 88:239–246

35. Frisch MJ, Trucks GW, Schlegel HB, Scuseria GE, Robb MA, Cheeseman JR, Scalmani G, Barone V, Mennucci B, Petersson GA, Nakatsuji H, Caricato M, Li X, Hratchian HP, Izmaylov AF, Bloino J, Zheng G, Sonnenberg JL, Hada M, Ehara M, Toyota K, Fukuda R, Hasegawa J, Ishida M, Nakajima T, Honda Y, Kitao O, Nakai H, Vreven T, Montgomery JA, Peralta JE, Ogliaro F, Bearpark M, Heyd JJ, Brothers E, Kudin KN, Staroverov VN, Kobayashi R, Normand J, Raghavachari K, Rendell A, Burant JC, Iyengar SS, Tomasi J, Cossi M, Rega N, Millam JM, Klene M, Knox JE, Cross JB, Bakken V, Adamo C, Jaramillo J, Gomperts R, Stratmann RE, Yazyev O, Austin AJ, Cammi R, Pomelli C, Ochterski JW, Martin RL, Morokuma K, Zakrzewski VG, Voth GA, Salvador P, Dannenberg JJ, Dapprich S, Daniels AD, Farkas O, Foresman JB, Ortiz JV, Cioslowski J, Fox DJ (2009) Gaussian 09, Revision B.01
36. Zhao Y, Truhlar DG (2008) The M06 suite of density functionals for main group thermochemistry, thermochemical kinetics, noncovalent interactions, excited states, and transition elements: two new functionals and systematic testing of four M06-class functionals and 12 other functionals. Theor Chem Acc 120:215–241
37. Boys SF, Bernardi FD (1970) The calculation of small molecular interactions by the differences of separate total energies. Some procedures with reduced errors. Mol Phys 19:553–566
38. Diao G, Zhou W (2004) The electrochemical behavior of p-sulfonated calix [4] arene. J Electroanal Chem 567:325–330
39. Bocarsly AB, Gibson QD, Morris AJ, L'Esperance RP, Detweiler ZM, Lakkaraju PS, Zeitler EL, Shaw TW (2012) Comparative study of imidazole and pyridine catalyzed reduction of carbon dioxide at illuminated iron pyrite electrodes. ACS Catal 2:1684–1692
40. Ashwin BM, Vinothini A, Stalin T, Muthu Mareeswaran P (2017) Synthesis of a safranin T - p-sulfonatocalix[4]arene complex by means of supramolecular complexation. Chem Select 2:931–936
42. Ashwin BM, Saravanan C, Senthilkumaran M, Sumathi R, Suresh P, Muthu Mareeswaran P (2017) Spectral and electrochemical investigation of p-sulfonatocalix[4]arene stabilized vitamin E aggregation. Supramol Chem. doi:10.1080/10610278.2017.1351612